Journal of Organometallic Chemistry 694 (2009) 1297–1307

Contents lists available at ScienceDirect

Journal of Organometallic Chemistry

journal homepage: www.elsevier.com/locate/jorganchem

Density functional studies on chromium catalyzed ethylene trimerization

Sumit Bhaduri [a], Sami Mukhopadhyay [b,*], Sudhir A. Kulkarni [b]

[a] Reliance Industries Limited, Swastik Mill Compound, V.N. Purav Marg, Chembur, Mumbai 400 071, India
[b] VLife Sciences Technologies Private Limited, Pride Purple Coronet, 1st Floor, Survey No. 287, Baner Road, Pune 411 045, India

ARTICLE INFO

Article history:
Received 6 October 2008
Received in revised form 25 November 2008
Accepted 4 December 2008
Available online 16 December 2008

Keywords:
Density functional
Cationic
Chromium(II)/chromium(IV) catalyst
Metallacycle mechanism
Cossee mechanism
Ethylene trimerization

ABSTRACT

Mechanism of ethylene trimerization using chromium catalyst is investigated using density functional methods. Recent experimental results indicate Cr-based homogeneous catalysts to follow metallacycle pathway in ethylene tri-, teta- and oligomerization reactions. Given the importance of chlorinated Cr-based active catalysts in these reactions, we have used "bare" minimal ligands like Cl^- and considered catalytic cycles with neutral or cationic intermediates starting with $[Cr(II)Cl_2(ethylene)_2]$ and $[Cr(II)Cl(ethylene)_2]^+$, respectively. We have compared both 'Cossee' and the 'metallacycle' mechanisms on these model systems utilizing density functional computations at B3LYP/LANL2DZ(d,p) level. The metallacycle mechanism with cationic Cr(II)–Cr(IV) intermediates is found to be the most favored path, with oxidative coupling of two coordinated ethylene to form the chromacyclopentane being the rate determining step (RDS). We also found that with neutral intermediates the Cossee pathway rather than the metallacycle mechanism is followed. Thus in spite of the simplicity of using just Cl^- as ligand in the model catalytic intermediates, our computational results match remarkably well with many recent and important experimental findings.

1. Introduction

Linear α-olefins (LAOs) like 1-hexene, 1-octene are used as comonomers in commercial production of linear low density polyethylene. These linear α-olefins are produced commercially by ethylene oligomerization catalysts which are non-selective, and yield a mixture of LAOs whereas more selective routes are industrially desirable. More selective route for trimerization of ethylene to 1-hexene using Cr catalysts is a well known innovation utilized by different technologies such as Phillips pyrrolide system [1–5], BP diphosphine system [6,7], and Sasol mixed heteroatomic system [8–12].

Recently, the mechanistic aspects of ethylene tri- and tetramerization with Cr catalysts have attracted considerable attention. Recent reviews on ethylene trimerization from Dixon and Morgan's group [13] and on ethylene tri- and tetra-merization by Wass [14] are noteworthy. A variety of homogeneous [15–26] and heterogeneous [27] Cr catalysts with different ligands have been reported. The essential mechanistic steps involve active catalyst that is generated in situ by the addition of a suitable co-catalyst (e.g. methylaluminoxane, MAO) which acts as a ligand abstractor and deprotonator [7,20,21,28–33] to generate cationic Cr(II)/Cr(IV) and/or neutral Cr(I)/Cr(III) species [7,20,21,28,30,33,34–40]. As shown in Scheme 1, the chromacyclopentane, arising from oxidative coupling of two co-ordinated ethylene molecules to active Cr catalyst, is a crucial structure and the starting point for two different pathways, the "metallacycle" or the Cossee [41,42] mechanism as detailed below.

From the mechanistic point of view, the use of deuterium labeling techniques support involvement of metallacycle mechanism [14,26,28,43,44]. For example, catalytic trimerization of a 1:1 mixture of C_2D_4 and C_2H_4 using Cr–PNP-based catalytic systems give isotopologs of 1-hexene without H/D scrambling and provide unequivocal support for the metallacycle mechanism [7,28]. The detailed mechanistic steps that are of significance in the context of selective trimerization of ethylene are shown in Scheme 2a, involving the formation of chromacyclopentane, followed by co-ordination of an ethylene molecule and subsequent expansion of the chromacyclopentane to chromacycloheptane whose well characterized single crystal X-ray structures are also known [45,46]. The labeling results also support a mechanism of 1-hexene formation from a chromacycloheptane via a concerted 3,7-H shift which bypasses the formation of a chromium hydride by stepwise β-H elimination [28] (cf. Scheme 2a). For other PNP ligated selective tetramerization Cr-catalysts, a similar extended metallacycle mechanism has been shown to operate [43,44]. These experimental facts therefore clearly indicate the ubiquitous presence of the metallacycle pathway irrespective of the complexities of the Cr-based catalytic systems involved in selective tri- or tetramerization [14,28,43,44], oligomerization [22,23,26] and also polymerization [27] reactions.

* Corresponding author. Tel./fax: +91 20 27291590/91.
E-mail addresses: sumit_bhaduri@ril.com (S. Bhaduri), samim@vlifesciences.com (S. Mukhopadhyay), sudhirk@vlifesciences.com (S.A. Kulkarni).

0022-328X/$ - see front matter © 2008 Elsevier B.V. All rights reserved.
doi:10.1016/j.jorganchem.2008.12.012

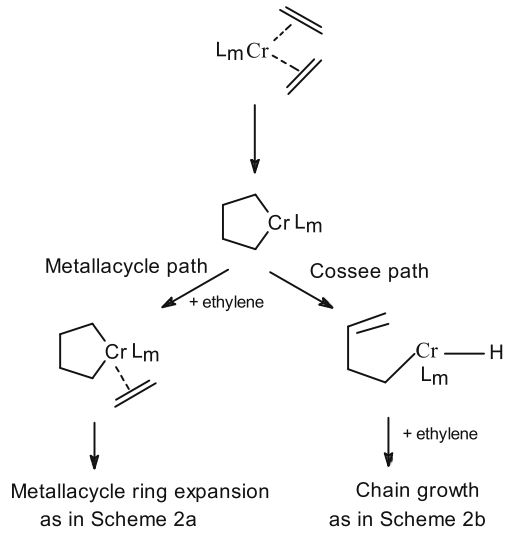

Scheme 1. Implication of chromacyclopentane in both metallacycle and Cossee pathways for ethylene trimerization.

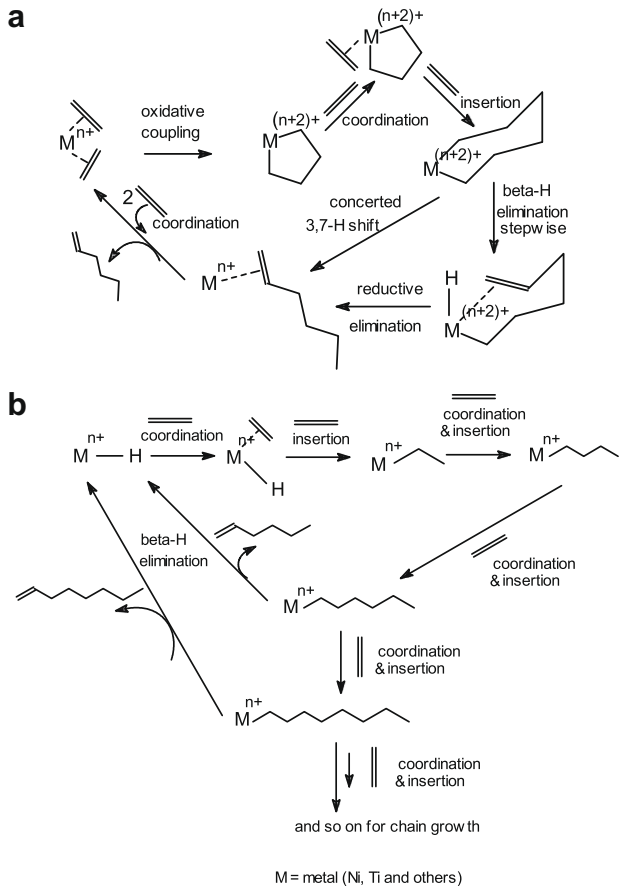

Scheme 2. (a). Metallacycle pathway for ethylene trimerization. (b). Cossee pathway for ethylene tri-, oligo- and polymerization.

This is in contrast to the dominant Cossee mechanism (Scheme 2b) for the Ti-based polyethylene manufacture, or the Ni-based SHOP process [47,48]. The standard nickel oligomerization (SHOP) catalyst, gives a broader distribution of 1-hexene isotopologs with H/D scrambling which is consistent with the Cossee-type mechanism of Scheme 2b, and indicates the involvement of metal hydride intermediates.

In McGuinness et al.'s recent experimental work involving Cr(III) catalysts of bis(carbene)pyridine ligands together with MAO, the mechanism of ethylene oligomerization chain growth was shown to be ligand dependent, with high activity and selectivity resulting only for those catalysts which support a metallacycle mechanism [26]. For example, for bidentate carbene–pyridine and carbene–thiophene ligands, it was found that the mechanism switched from metallacycle to Cossee-Arlman type linear chain growth which led to very poor activity.

Much of the recent research is also geared towards finding out whether in Cr-catalyzed selective tri- or tetramerization, cationic or neutral species are more likely to be involved as catalytic intermediates [7,20,28–30]. Among cationic and neutral complexes derived from the Cr–PNP combination, the former has been found to be active towards the trimerization of ethylene and 2-butyne but not the latter [28]. Studies with different PNP and SNS type ligand based Cr(II) and Cr(III) catalysts indicate that the catalytically active species are formally cationic, and the catalytic cycle involves cationic Cr(II)–Cr(IV) rather than neutral Cr(I)–Cr(III) intermediates i.e., $n = 2$ in Scheme 2a [20,30]. However, as there are experimental evidence for both Cr(I)/Cr(III) [7,31] and Cr(II)/Cr(IV) [32,33,49] mechanisms, the oxidation state of Cr in the catalytic cycle must be ligand dependent [20]. Further, the role of the Cr spin states in all the intermediates of the proposed catalytic cycle for ethylene tri- and tetramerization [34] has also been explored.

In a recent DFT study on the mechanism of Cr catalyzed ethylene trimerization, Janse van Rensburg et al showed that the metallacycle mechanism is followed to yield 1-hexene [49] for the famous Phillips Cr-catalyst system. This involved Cr(II)/Cr(IV) species starting from a catalytically active Cr(II) intermediate using pyrrolate and Cl/ $ClAlMe_3$ anionic ligands and the metallacycle growth step was found to be the rate determining step.

The other recent computational studies [50–53] that are of relevance, deal with Ta and Ti-based ethylene trimerization systems [54–58]. They attempt to explain (i) preference of insertion of the third ethylene molecule into the metallacyclopentane over the liberation of 1-butene and (ii) preference of 1-hexene liberation over metallacycle growth [13,14]. The reductive 1-hexene elimination process of Scheme 2a, involving metal mediated, agostic-assisted concerted 3,7-H shift also finds support from recent computational studies [49,50–53,59–61]. The concerted mechanism is found to be energetically more favorable than a stepwise mechanism for titanium, tantalum, and chromium [43,44,62] ethylene trimerization systems.

With these extensive background studies, the work reported here was undertaken with a view to rationalize some of the key experimental observations by using computational (DFT) methodologies. Thus taking ethylene trimerization as the model reaction, we address the following specific questions: First, do theoretical calculations show unequivocally that in terms of the reaction energetics, rather than the Cossee mechanism (Schemes 3 and 4), whether the metallacycle mechanism (Scheme 5) is the preferred one for chain growth? Considering the experimental evidence for the involvement of Cr based metallacycle pathways for selective tri- or tetramerization [14,28,43,44], oligomerization [22,23,26] and polymerization [27] reactions, this question is of considerable importance.

Second, how important is it to have positively charged and co-ordinatively unsaturated catalytic intermediates? The co-catalyst indeed has significant influence on activity and selectivity, but more importantly they are known to help the generation of positively charged and co-ordinatively unsaturated catalytic intermediates through the abstraction of an anionic ligand [7,20,21,24,28–33,63]. However, with heterogeneous Cr-catalyst no co-catalyst is required. Co-catalyst induced creation of co-ordinative unsaturation and cationic metal centers in heterogeneous

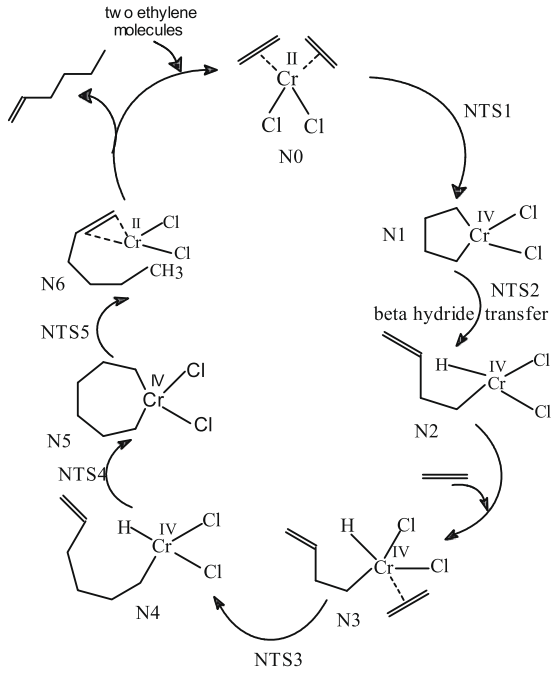

Scheme 3. Cossee-type reaction pathway for ethylene trimerization on neutral model system, $[Cr(II)Cl_2(ethylene)_2]$.

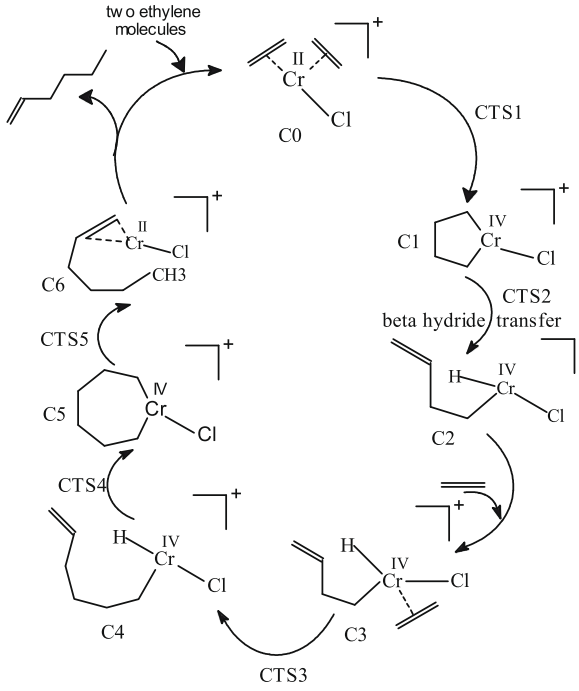

Scheme 4. Cossee type reaction pathway for ethylene trimerization on cationic model, $[Cr(II)Cl(ethylene)_2]^+$.

Cr-catalyst can therefore be ruled out. With this background, it is important therefore to know if neutral (Scheme 3) or cationic intermediates (Schemes 4 and 5) make a significant impact on the mechanism of ethylene trimerization.

In our simple model system, we have considered chlorides as ligands and investigated the energetics of catalytic cycles initiated by both the neutral and the cationic model intermediates, $[Cr(II)Cl_2(ethylene)_2]$ and $[Cr(II)Cl(ethylene)_2]^+$. These intermediates could possibly be the active species in the experimentally well

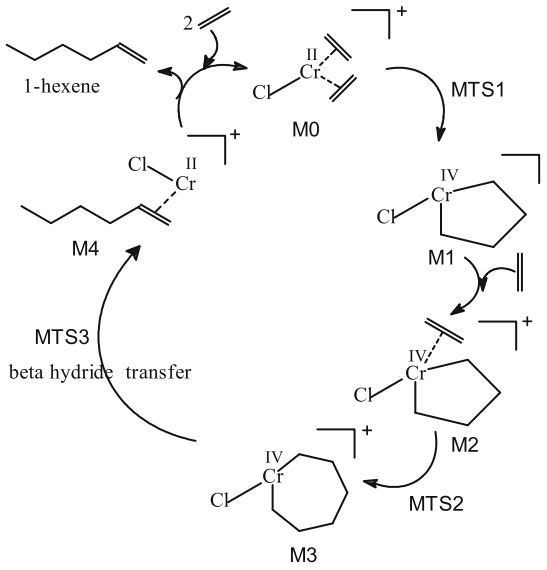

Scheme 5. Usual metallacycle pathway for ethylene trimerization on cationic model, $[Cr(II)Cl(ethylene)_2]^+$.

known effective ethylene oligomerization "bare" $[CrCl_3(thf)_3]$ catalyst in combination with MAO or mixture of $AlEt_3$ and $[Ph_3C][BAr^F_4]$, that leads to Schulz-Flory distribution of α-olefins [21,26]. We have studied the ethylene di- and tri-merization as the first two fundamental steps in the entire pathway for ethylene oligomerization. One of the reasons for choosing simple chloride ligand in our model systems is the importance of chlorinated Cr based active catalysts in ethylene tri-, tetra-merization and oligomerization reactions [25]. Blom et al.'s recent DFT investigations [25] on ethylene trimerization revealed that chlorinated Cr-catalyst favors the trimerization process over non-chlorinated catalyst by significant lowering of activation energy barriers for the key steps of chromacyclopentane formation and 1-hexene liberation for the chlorinated catalyst [25]. The relative energies of intermediates and transition states of Cossee [41,42] (cf. Schemes 3 and 4) and metallacycle mechanisms [44,49] (cf. Scheme 5) have been investigated keeping the literature reported experimental evidences in focus. We have considered the important aspect of co-catalyst induced co-ordinative unsaturation and cationization in our cationic model system, $[Cr(II)Cl(ethylene)_2]^+$ with one chloride removed from the co-ordination sphere of the neutral model.

2. Methodology

The catalytic cycles modeled in this work are shown in Schemes 3–5. Chromium is formally in 2+ oxidation state in the starting bis-olefin complex and also in the final 1-hexene bound complex. The oxidation state of the metal ion is formally 4+ throughout the rest of the structures in the Cossee(C) mechanism (cf. Schemes 3 and 4) and the metallacycle mechanism (cf. Scheme 5). This is similar to the Cr oxidation states considered in earlier DFT studies by other groups [25,49] involving the usual metallacycle pathway.

All the geometries have been obtained using hybrid density functional method B3LYP [64–66] (three parameter Becke's exchange energy functional along with correlation functional due to Lee, Yang and Parr). Throughout all calculations, we have used the extended basis set including diffuse and polarization functions to LANL2DZ basis for C, H and Cl atoms and will be designated as LANL2DZ(d,p) basis herein after [67]. The LANL2DZ basis set used includes a double zeta valence basis set (8s5p5d)/[3s3p2d] for Cr with the Hay and Wadt ECP replacing core electrons up to 2p

and Huzinaga-Dunning (D95) double zeta basis set for all other atoms. The LANL2DZ basis has been well known to be utilized in several studies on organometallic systems as well as chromium complexes [68].

The vibrational frequencies and zero point energies (ZPE) of all the stationary points have been obtained on the potential energy surface (PES) of ethylene polymerization for the catalysts described above at LANL2DZ(d,p) levels. The convergence criteria during optimization of all structures was set at a threshold of 0.0003 a.u. for RMS Force and at a threshold of 0.0012 a.u. for RMS displacement. The quadratic convergence criteria was chosen for optimizations of structures wherever normal optimization were not successful.

The magnitude of imaginary frequency and corresponding eigenvectors were analyzed for all transition states to verify involvement of required atoms. All transition states were further verified using Intrinsic Reaction Co-ordinate (IRC) calculations that actually indicates that the transition state is directly connected to the corresponding reactant and product intermediates.

All our calculations have been performed using the program GAUSSIAN 98 [69].

3. Results and discussion

For the ethylene trimerization reaction we have evaluated the likelihood of chain growth by the metallacycle or the Cossee mechanism [41,42]. We have used $[Cr(II)Cl(ethylene)_2]^+$ and $[Cr(II)Cl_2(ethylene)_2]$ as cationic and neutral model complexes, respectively. It is well known that though the formal oxidation state of Cr depends on the specific ligands used, in a large number of cases based on experimental evidence, Cr(II)/Cr(IV) is suggested to be involved in the catalytic cycle [7,20,21,28,30,32,33,49]. Hence we have considered the Cr(II)/Cr(IV) oxidation states in our work with both singlet and triplet states. The reaction energies of $[Cr(II)Cl_2(C_2H_4)_2]$ to $[Cr(IV)Cl_2(C_4H_8)]$ (Scheme 3, N0–N1) steps were compared for both singlet and triplet spin states of Cr. All these reactions are found to be endothermic with minimum endothermicity for the singlet Cr(II)–Cr(IV) conversion. Hence, Chromium in all of the structures considered here is in the low spin state (singlet).

The nomenclatures used for the different structures and transition states in Schemes 3–5 is as follows. The prefixes "N", "C" and "M" denote neutral, cationic and metallacycle pathways, while "TS" denotes transition states of the individual reaction steps in the catalytic cycle, respectively.

3.1. Structure and bonding aspects

3.1.1. Cossee pathway with neutral, $[Cr(II)Cl_2(ethylene)_2]$ model system

We have explored all the stationary structures (structures N0–N6) on the potential energy surface (PES) of the Cossee mechanism with neutral catalytic system as shown in Scheme 3. The corresponding optimized geometries are in Fig. 1. Here, Chromium is in distorted trigonal bipyramid environment in the Π-complex N3 and the transition states NTS2–NTS5 except NTS4. In all the rest of the structures, Cr is in distorted tetrahedral environment.

Comparison of the Cr–C=C (ethylene) and C=C (ethylene) bond distances indicate that Cr–ethylene Π-complexing interactions are stronger in N0 than in N3 (cf. Fig. 1). This is consistent with less electron density and hence Π-backbonding ability of Cr(IV) in N3 as compared to Cr(II) in N0.

In N6, the Cr–alkene interaction is more significant than in N0 due to the enclosed geometry of the complex, N6. This gets reflected in the longer C=C bond and corresponding Cr–C=C shorter distances (cf. Fig. 1). It may also be noted that while complex N6 has only one Π-bonded alkene, complex N0 has two ethylenes competing for Π-donation to Cr(II).

In the transition states NTS2 and NTS5 the emergent C=C bonds of the carbon chains are closer to Cr and the Cr–alkene interactions improve. These are reflected in the C=C bond distances within the range of 1.349–1.429 Å, and the Cr–C=C bond distances between 2.037 Å and 3.028 Å.

For NTS4, the C=C bond distance is 1.342 Å and the Cr–C=C bond distances are 4.545 Å and 4.492 Å, indicating negligible Cr–alkene interaction in NTS4. The C=C part in N4 is very far away from the Cr center (cf. Fig. 1). However, the C=C part can bend back to come closer to Cr in the NTS4 structure. This leads to a reorientation of Cr–C=C distances, and relatively close proximity of the hydride (Cr–H) with respect to the C=C carbons (3.078 Å, 2.955 Å). This facilitates the hydride shift from Cr to the β-carbon (C-6) and leads to the formation of the metallacycloheptane N5 (cf. Fig. 1).

The Cr(IV)–H distances in the intermediates N2–N4 and the TSs NTS2–NTS4 are all in the range of 1.524–1.548 Å, which are in accordance with those reported in the literature [70,71]. In the Cr(II)–1-hexene complex N6, the short $Cr(II)\cdots H(CH_3)$ distance, 1.977 Å and one long C–H bond of CH_3, 1.117 Å as against 1.098 Å each for the other two C–H bonds, are indicative of reasonable α-agostic stabilizing interactions. Also, in the corresponding transition state, NTS5, the short $Cr(II)\cdots H$ distance, 1.625 Å and corresponding one long $C\cdots H$ distance of α $-CH_2\cdots H\cdots Cr$, 1.467 Å, as against 1.096 Å, 1.130 Å for the other two C–H bonds of α-CH_2, indicate stabilization by α-agostic interactions (cf. Fig. 1). Similar agostics have already been reported in different model systems [49].

3.1.2. Cossee pathway with cationic, $[Cr(II)Cl(ethylene)_2]^+$ model system

We have explored all the stationary structures (C0–C6) on the potential energy surface (PES) of the Cossee mechanism with cationic catalytic system as shown in Scheme 4 and the corresponding optimized geometries as in Fig. 2. Here, Cr is in distorted tetrahedral environment in complexes C2–C4, and transition states CTS3–CTS5. In rest of the structures Cr is in distorted trigonal environment. This is in contrast to the distorted trigonal bipyramid and tetrahedral structures for the analogous neutral structures in Cossee pathway (cf. Fig. 1).

For structure C2, the C=C bond length is 1.396 Å and the Cr–C=C distances are 1.971 Å and 2.148 Å which indicate significantly increased Cr–ethylene interactions as compared to the neutral analog N2. This probably is due to the increased co-ordinative unsaturation in C2 as compared to N2 that allows the C=C part a closer approach to the Cr-center.

The Cr(IV)–H distances in the intermediates C2–C4, and the TSs CTS2–CTS4 are in the range 1.508–1.561 Å and for CTS5 it's the longest, 1.648 Å which are in accordance with those reported in the literature [70,71]. The overall structural features are broadly similar to those discussed for the Cossee path with the neutral model (cf. Figs. 1 and 2), but some salient differences are as follows.

The C=C part of the alkene chain is closer to Cr in CTS4 than in NTS4. The C=C bond lengths in C0 and C6 are both 1.393 Å, although the environment of the C=C part is significantly different in these two structures (cf. Fig. 2). This is in contrast to the corresponding neutral complexes N0 and N6 (vide supra). This may be due to the significant increase in the electrophilicity of Cr in the cationic system as compared to the neutral system.

The Cr–Cl distances for all the cationic model structures as well as distance of ethylene from Cr in C0 and C3 are shorter than that the corresponding neutral structures. This again is probably due to the increased positive charge.

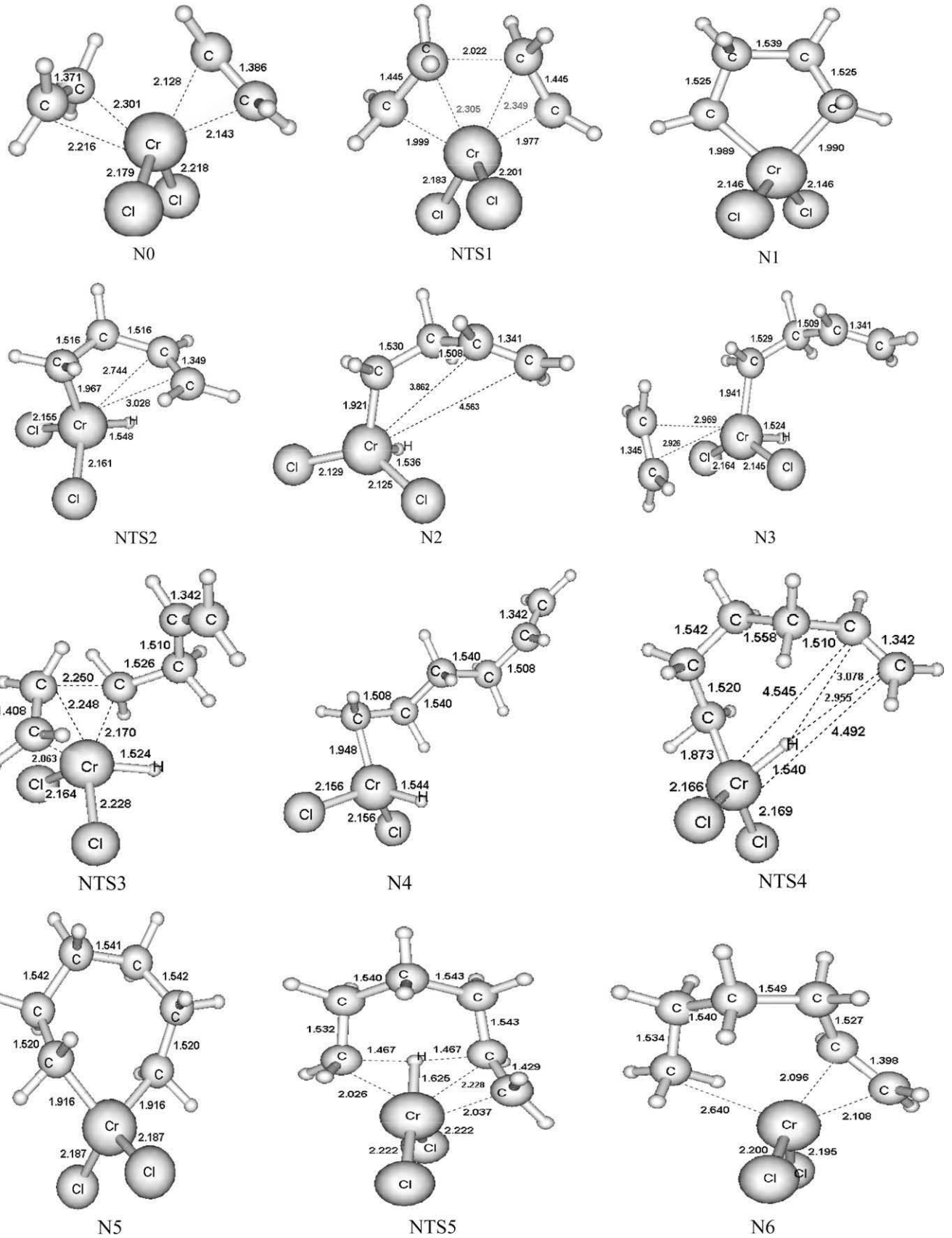

Fig. 1. Optimized geometries of all structures on the PES of ethylene trimerization using neutral [Cr(II)(C_2H_4)$_2$$Cl_2$] (N0) active catalyst at B3LYP/LANL2DZ(d,p) level for Cossee type reaction pathway. Bond lengths are in Å. All the structures have been visualized by using MDS 3.5 molecular modeling software [72].

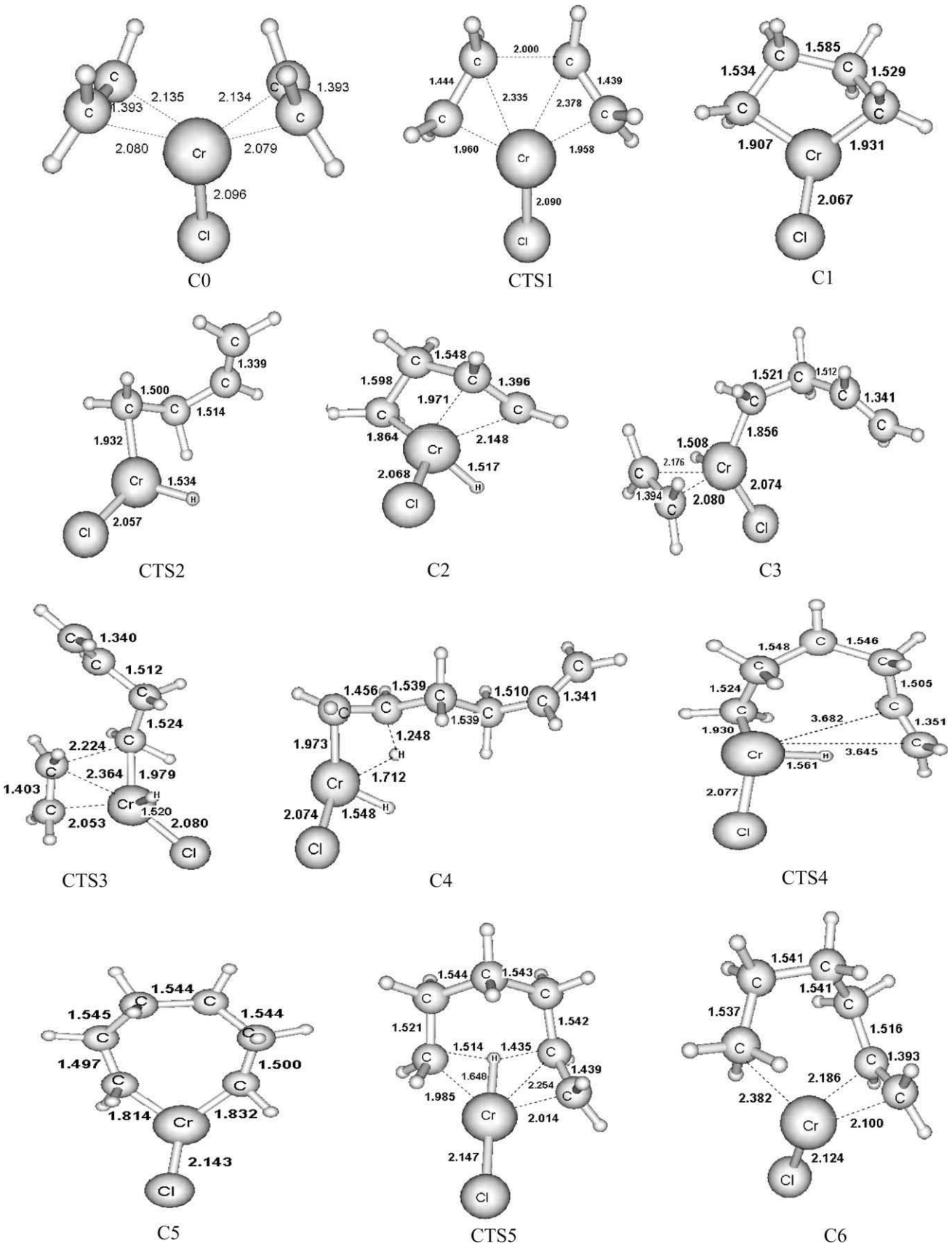

Fig. 2. Optimized geometries of all structures on the PES of ethylene trimerization using cationic $[Cr(II)(C_2H_4)_2Cl]^+$ (C0) active catalyst at B3LYP/LANL2DZ(d,p) level for Cossee type reaction pathway. Bond lengths are in Å.

In C4, there is a significant agostic interaction between Cr and β-H (H atom on C-3) of the growing olefin chain. This is evident from the short Cr(IV)···H(β-CH_2) distance, 1.712 Å, and one long C–H bond of β-CH2, 1.248 Å as against 1.099 Å for the other C–H bond. Such β-agostic interaction is absent in the corresponding neutral structure N4.

Similarly, α-agostic stabilizing interactions are seen in the Cr(II) ethylene complex (C6) and the transition state, CTS5.

3.1.3. Metallacycle pathway with neutral and cationic model systems

While systematically exploring all the probable reaction mechanisms, we tried computations on the catalytic cycle that starts with neutral [Cr(II)Cl_2(ethylene)$_2$] and proceeds by the metallacycle pathway. However, all our attempts for locating the ethylene Π-complexes of metallacyclopentane and also metallacycloheptane resulted in the ethylene drifting away from the Cr(IV) center and the corresponding transition states going back to the starting metallacycles. Similar ethylene drifts have also been observed and reported for Cr-catalyzed ethylene tri- and tetramerization based computational studies [49,63]. These results were reproduced for both Cr(IV) triplet and singlet spin states, indicating that the usual metallacycle mechanism(cf. Scheme 2a) can not be operative. We have therefore explored the metallacycle pathway where only cationic intermediates are involved (cf. Scheme 5).

Most of the intermediates and transition states in this metallacycle pathway are same as those in the cationic Cossee pathway (cf. Scheme 4), that have already been covered in the preceding section and will not be discussed any further. However, although M0, M1, M3, M4, MTS1 and MTS3 are identical with C0, C1, C5, C6, CTS1 and CTS5, respectively, for unambiguous description of reaction mechanisms, the M-prefixed designations have been used. Only two new structures, the ethylene bound complex M2 and the transition state, MTS2 of the metallacycle pathway will be discussed (cf. Scheme 5, Fig. 3).

Cr is in distorted tetrahedral environment in the intermediate M2 and the transition state MTS2, MTS3 (cf. Fig. 3). The ethylene bound complex M2 is formed upon ethylene addition to the cationic chromacyclopentane, M1. This again may be rationalized on the basis of increased positive charge, i.e., electrophilicity, of M1 and the absence of one bulky chloride ligand. In M2, there are significant Cr–ethylene interactions, the C=C bond of ethylene is elongated to 1.387 Å from 1.340 Å in free ethylene. Also, the Cr–C=C (ethylene) bond lengths are significantly shorter (2.107 Å, 2.182 Å).

As expected in MTS2, the C=C bond of ethylene is further elongated to 1.411 Å, and the Cr–C=C (ethylene) bond distances are 2.039 Å and 2.332 Å. In going from M2 to MTS2, the C–C distance between one terminal of the ethylene to the α-C of the chromacyclopentane significantly shortens from 3.006 Å to 2.135 Å, while the corresponding Cr–α-C bond elongates from 1.991 Å to 2.096 Å. These changes clearly exemplify the different dynamic structural readjustments that happen in a concerted fashion from ethylene bound complex M2 to the corresponding transition state MTS2 leading finally to chromacycloheptane, M3. Similar results are reported earlier for Cr-pyrrole, Cl/ClAlMe$_3$ neutral model systems for ethylene trimerization [49].

3.2. Energetics

The zero point energy (ZPE) corrected relative energies (*E* in kcal/mol) of stationary points on the PES of ethylene trimerization on Cossee and metallacycle pathways at B3LYP/LANL2DZ(d,p) level are given in Tables 1–3 and the corresponding relative energy diagrams are as shown in Figs. 4 and 5. These energy values reveal the following trends.

Table 1
Zero point energy (ZPE) corrected relative energies (kcal/mol) of stationary points on the PES of ethylene trimerization using neutral [Cr(II)(C_2H_4)$_2$$Cl_2$] (N0) active catalyst at B3LYP/LANL2DZ(d,p) level[a] for Cossee reaction pathway.

Structures	E[b]	E_{act}[c]
N0	0.00	
NTS1	22.09	22.09
N1	7.29	
NTS2	36.62	29.33
N2	31.09	
N3	31.21	
NTS3	51.17	19.97
N4	9.29	
NTS4	12.13	2.84
N5	−15.74	
NTS5	−0.45	15.29
N6	−26.48	

[a] Total ZPE corrected energies (electronic + ZPE in a.u.) calculated at B3LYP/LANL2DZ(d,p) level (LANL2DZ(d,p) = LANL2DZ + diffuse and polarization functions for C, Cl, H) of structures are: N0 = −273.385815; N1 = −273.374196; N2 = −273.336272; N3 = −351.884932; NTS3 = −351.853112; N5 = −351.959738; NTS5 = −351.935381; N4 = −351.919848; NTS1 = −273.350611; NTS4 = −351.915330; N6 = −351.976862; NTS2 = −273.327453; N7 = −430.529126; C_2H_4 = −78.548846.

[b] *E* is ZPE corrected relative energy in kcal/mol: for N1–N2, NTS1, NTS2 relative to N0; for N3, NTS3, NTS4, NTS5, N5, N6, N4 relative to N0 + one ethylene (−351.934661 a.u.).

[c] E_{act} is activation barrier in kcal/mol.

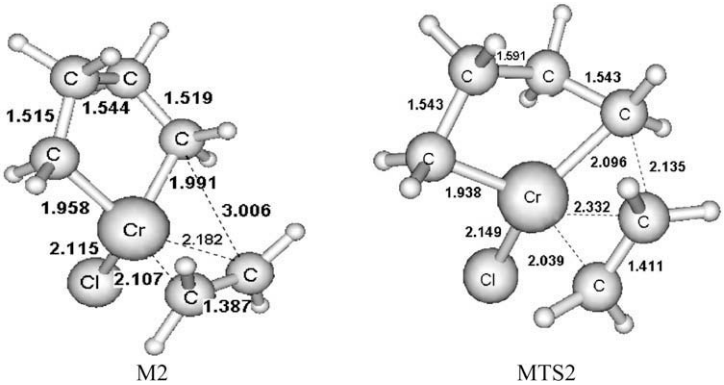

Fig. 3. Optimized geometries of all structures on the PES of ethylene trimerization using cationic [Cr(II)(C_2H_4)$_2$Cl]$^+$ (M0) active catalyst at B3LYP/LANL2DZ(d,p) level for metallacycle reaction pathway. Bond lengths are in Å. Most of the structures in this Figure for metallacycle pathway (cf. Scheme 5) are same as those in the cationic Cossee pathway (cf. Scheme 4) and are already presented in Fig. 2. M0, M1, M3, M4, MTS1 and MTS3 are identical with C0, C1, C5, C6, CTS1 and CTS5, respectively, as in Fig. 2. Hence only the structures M2 and MTS2 are shown here.

Table 2
Zero point energy (ZPE) corrected relative energies (kcal/mol) of stationary points on the PES of ethylene trimerization using cationic $[Cr(II)(C_2H_4)_2Cl]^+$(C0) active catalyst at B3LYP/LANL2DZ(d,p) level[a] for Cossee reaction pathway.

Structures	E[b]	E_{act}[c]
C0	0.00	
CTS1	24.53	24.53
C1	16.35	
CTS2	48.87	32.52
C2	23.38	
C3	14.08	
CTS3	31.33	17.25
C4	22.72	
CTS4	25.23	2.51
C5	−4.59	
CTS5	−0.56	4.03
C6	−21.03	

[a] Total ZPE corrected energies (electronic + ZPE in a.u.) calculated at B3LYP/LANL2DZ(d,p) level (LANL2DZ(d,p) = LANL2DZ + diffuse and polarization functions for C, Cl, H) of structures are: C0 = −258.105139; CTS1 = −258.066047; C1 = −258.079087; C5 = −336.661295; C6 = −336.687492; CTS5 = −336.654877; CTS2 = −258.027262; C2 = −258.067886; C3 = −336.631555; C4 = −336.617775; CTS3 = −336.604052; CTS4 = −336.613780; C_2H_4 = −78.548846.
[b] E is ZPE corrected relative energy in kcal/mol: for C1, C2, CTS1, CTS2 relative to C0; for C3, CTS3, C4, C5, C6, CTS5 relative to C0 + one ethylene (− 336.653985 a.u.).
[c] E_{act} is activation barrier in kcal/mol.

Table 3
Zero point energy (ZPE) corrected relative energies (kcal/mol) of stationary points on the PES of ethylene trimerization using cationic $[Cr(II)(C_2H_4)_2Cl]^+$ (M0) active catalyst at B3LYP/LANL2DZ(d,p) level[a] for metallacycle reaction pathway.

Structures	E[b]	E_{act}[c]
M0	0.00	
MTS1	24.53	24.53
M1	16.35	
M2	−10.33	
MTS2	5.09	15.42
M3	−4.59	
MTS3	−0.56	4.03
M4	−21.03	

[a] Total ZPE corrected energies (electronic + ZPE in a.u.) calculated at B3LYP/LANL2DZ(d,p) level (LANL2DZ(d,p) = LANL2DZ + diffuse and polarization functions for C, Cl, H) of structures are: M0 = −258.105139; MTS1 = −258.066047; M1 = −258.079087; M2 = −336.670445; M3 = −336.661295; M4 = −336.687492; MTS2 = −336.645880; MTS3 = −336.654877; C_2H_4 = −78.548846.
[b] E is ZPE corrected relative energy in kcal/mol: for M1, MTS1 relative to M0; for M2, MTS2, M3, M4, MTS3 relative to M0 + one ethylene (− 336.653985 a.u.).
[c] E_{act} is activation barrier in kcal/mol.

3.2.1. Cossee pathway with cationic and neutral model systems

There are similar overall trends in energy changes for both the neutral, and the cationic, mechanistic models following the Cossee pathway (cf. Schemes 3 and 4). The conversions of the bis-ethylene complexes N0 and C0 to the corresponding metallacyclopentanes, N1 and C1, are endothermic reactions by 7.30 kcal/mol and 16.35 kcal/mol, respectively (cf. Tables 1 and 2, Figs. 1, 2, 4 and 5). The formal oxidative coupling of two ethylene molecules take place via transition states NTS1 and CTS1 with activation energy barriers of 22.09 kcal/mol and 24.53 kcal/mol, respectively.

The conversions of N1 and C1 to the corresponding β-H transferred intermediates N2 and C2 are also energetically uphill reactions with activation barriers of 29.33 and 32.52 kcal/mol, respectively. It is observed that the activation barrier for cationic C1–C2 conversion is higher by about 3.19 kcal/mol than that for the corresponding neutral N1–N2 conversion. This is because N1 and NTS2 are slightly more stabilized than C1 and CTS2.

The extra stabilization of NTS2 is probably due to increased Cr–alkene interactions since the C=C part is bent back closer to Cr in neutral NTS2 than in CTS2 (cf. Figs. 1 and 2). The relative energies

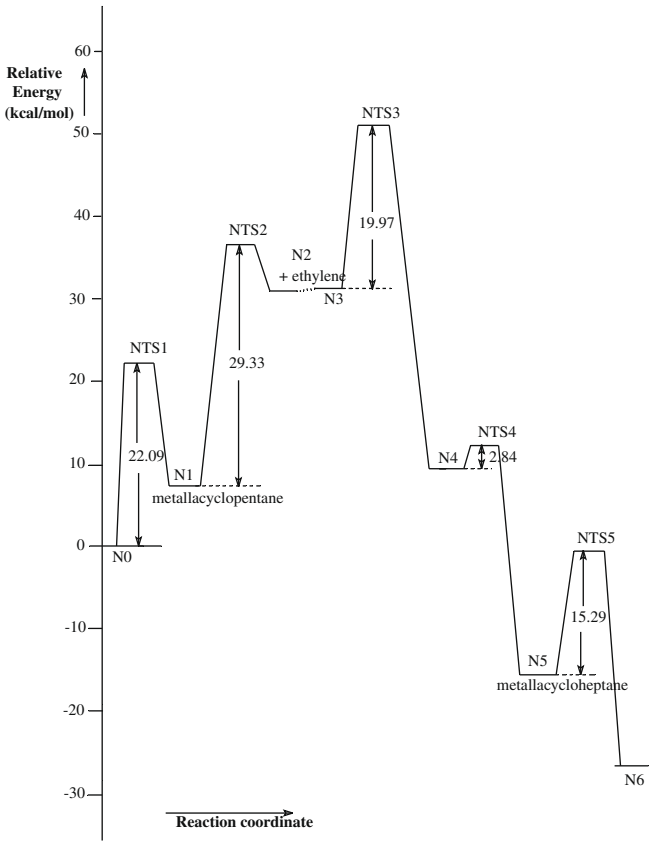

Fig. 4. Relative energy profile for ethylene trimerization using neutral $[Cr(II)(C_2H_4)_2Cl_2]$ (N0) active catalyst at B3LYP/LANL2DZ(d,p) level for Cossee type reaction pathway.

of N2 and C2 are 31.09 kcal/mol and 23.38 kcal/mol, respectively (cf. Tables 1 and 2). This significant stabilization of C2 compared to N2 is again due to increased Cr–alkene interactions as the C=C part of the carbon chain is bent back closer to Cr in cationic C2 than in neutral N2 (cf. Figs. 1 and 2).

The catalytic intermediates N1 and C1 are more stable than the succeeding ones N2 and C2 by 23.8 kcal/mol and 7.03 kcal/mol, respectively. The third ethylene molecule next gets added to these intermediates to form N3 or C3. The intermediate N3 is very close in energy to that of N2 (cf. Fig. 4). However, for the corresponding cationic C2–C3 conversion, there is a significant stabilization of around 9.3 kcal/mol (cf. Fig. 5). This stabilization can be rationalized on the basis of increased Cr–ethylene interactions as is evident from the corresponding structural changes discussed earlier.

The subsequent conversion of N3 or C3 to the intermediate N4 or C4 by the insertion of ethylene into the Cr–C bond occurs via the transition state NTS3 or CTS3, respectively. However, while N3–N4 is exothermic by 21.92 kcal/mol, C3–C4 is endothermic by 8.64 kcal/mol. The activation barriers of N3–N4 and C3–C4 are 19.97 kcal/mol and 17.25 kcal/mol, respectively (cf. Tables 1 and 2 and Figs. 4 and 5).

The conversions of intermediates N4 or C4 to the corresponding metallacycloheptane intermediates N5 or C5 occurs via hydride transfer to C-6, and the formation of C-7 to Cr bond. Both the transition states NTS4 and CTS4 are tetrahedral with low activation barriers of 2.84 kcal/mol and 2.51 kcal/mol, respectively. The N4–N5 and C4–C5 conversions are both exothermic by 25.03 kcal/mol and 27.31 kcal/mol, respectively. From the PES mapped by the IRC calculations, it was found that NTS4 and CTS4 are directly connected to N4, N5 and C4, C5, respectively. The corresponding

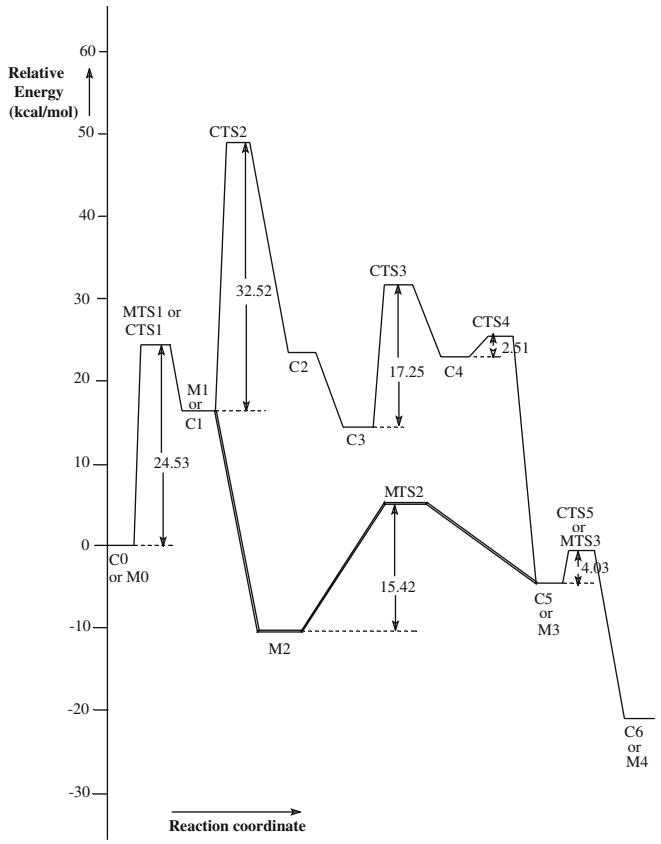

Fig. 5. Relative energy profile for ethylene trimerization using cationic $[Cr(II)(C_2H_4)_2Cl]^+$ (C0) active catalyst for Cossee type reaction pathway (bold line) and also using cationic $[Cr(II)(C_2H_4)_2Cl]^+$ (M0) active catalyst for metallacycle reaction pathway (bold line). Both pathways are computed at the same B3LYP/LANL2DZ(d,p) level. Please note that the first three and last three structures are common for both pathways.

structure and relative energetics of NTS4, CTS4 indicate that they are early TSs which rationalizes their low activation barriers.

In steps that precede the elimination of 1-hexene, the chromacycloheptanes N5 and C5 are converted to the intermediates N6 and C6. The transition states NTS5 or CTS5 associated with these conversions have activation barriers of 15.29 kcal/mol and 4.03 kcal/mol, respectively. The exothermicity of N5–N6 and C5–C6 are 10.74 kcal/mol and 16.44 kcal/mol, respectively. It may be noted that these reactions for both the neutral and the cationic system are reductive elimination reactions where the formal oxidation state of Cr changes from four to two. The change in the oxidation state of Cr is caused by a hydride transfer from the 3-CH_2 position to the 7-CH_2 position of the metallacycle framework. This leads to the formation of Π-co-ordinated 1-hexene and the 3,7-H shift occurs in a fully concerted fashion through the intermediacy of Cr (cf. Schemes 3 and 4). This type of concerted metal assisted hydride shift in metallacycloheptanes are well precedented in computational works on Cr, Ti, and Ta systems [13,14,49,50–53,59–61].

The stabilizing α-agostic interaction and the significant Π interactions in N6 and C6 (discussed earlier), make them the most stable intermediate in their respective catalytic cycles, with relative energies −26.48 kcal/mol and −21.03 kcal/mol. In our model mechanistic schemes 1-hexene elimination from N6 and C6, and subsequent additions of two ethylene molecules to $Cr(II)Cl_2$ and $[Cr(II)Cl]^+$, regenerate the starting bis-ethylene complexes N0 and C0 (cf. Schemes 3 and 4).

From the relative energy values it is clear that conversions of the metallacyclopentanes N1 and C1 to the corresponding β-H transferred structures N2 and C2 are associated with highest activation energy barriers of 29.33 kcal/mol and 32.52 kcal/mol, respectively. In other words for the Cossee mechanism involving either neutral or cationic intermediates, these are expected to be the rate determining steps. The high activation barriers may be attributed to geometrical constraints of chromacyclopentanes (N1 and C1) which also limit β-H–Cr interactions. This in turn prevents 1-butene elimination by a 3,5-H atom shift as has also been experimentally reported by Overett et al. [44]. Similar conclusions were drawn computationally for Ti and Ta catalyzed ethylene trimerization studies [13,14,50–53]. This is found to be due to the ring strain in metallacyclopentanes, as a result of which 1-butene liberation from them would actually have to proceed in a two-step mechanism requiring higher activation energies and reaction energies compared to metallacycle or chain growth and hence the growth pathway is favored over 1-butene elimination [13,14,50–53].

As reported by Overett et al. [44] for selective ethylene tetramerization the stabilization of the chromacycloheptane intermediate is crucial, as this allows the insertion of another ethylene molecule. In our model mechanistic cycles the net conversion of chromacyclopentanes (N1 and C1) to chromacycloheptanes (N5 and C5) can be considered as the following net reaction:

(i) N1 + ethylene → N5 or
(ii) C1 + ethylene → C5

The chromacycloheptanes N5 and C5 are more stable than the chromacyclopentanes N1 and C1 plus uncomplexed ethylene by −23.03 kcal/mol and −20.94 kcal/mol, respectively. Our results are thus consistent with what has been reported by others, i.e., the significant stabilization of a chromacycloheptane intermediate is an important driving factor for ethylene trimerization rather than 1-butene elimination [43,44].

3.2.2. Metallacycle pathway with neutral and cationic model systems

There is experimental evidence that indicate that in the Cr–PNP catalytic system, the rate determining step is the oxidative coupling of the first two ethylenes to form the metallacyclopentane intermediate as reported by Sasol group [44]. The recent DFT study by Janse van Rensberg et al. on Cr catalyzed ethylene trimerization, with a ligand framework consisting of pyrrole and chloride, identifies the conversion of chromacyclopentane to chromacycloheptane as the rate determining step [49]. However, our results mentioned above show that if the chromacyclopentane had to grow by the Cossee mechanisms, the catalytic cycle would involve intermediates such as N2 and C2, both of which have high kinetic barriers.

As discussed earlier, the neutral model system that starts with $[Cr(II)Cl_2(ethylene)_2]$, can not follow chain growth by the metallacycle pathway due to the instability of the ethylene adduct of chromacyclopentane. Thus reaction conditions under which neutral catalytic intermediates are more likely to be present, the Cossee mechanism (Scheme 3) is likely to be operative. As mentioned earlier in homogeneous catalytic systems an important role of the co-catalyst such as MAO is to generate co-ordinatively unsaturated cationic intermediates [7,20,21,24,28–33,63]. With heterogeneous chromium catalysts no co-catalysts are used and the complex mechanism is postulated to involve chain growth by Cossee as well as the metallacycle mechanisms [27], though the actual mechanism is still unresolved.

The metallacycle pathway works well when the cationic complex $[Cr(II)Cl(ethylene)_2]^+$ is used as the starting intermediate. The conversion of chromacyclopentane M1–M2 by ligation of one ethylene molecule is a barrierless process which is also exothermic by 26.68 kcal/mol (cf. Table 3, Fig. 5). Thus as is apparent from Fig. 5, among the two possibilities open to M1(≡C1), conversion

to either C2 or M2, the energetics overwhelmingly favor the latter. This implies that in situations where the reaction conditions promote the formation of cationic intermediates, the metallacycle mechanism for chain growth must dominate. Our results are thus consistent with what has been observed experimentally by isotope labeling studies [28].

The Π-complexed ethylene of M2 gets inserted in the chromacyclopentane via transition state MTS2 with an activation barrier of 15.42 kcal/mol leading to the chromacycloheptane, M3. This conversion of M2 to M3 is an endothermic process by 5.74 kcal/mol (cf. Fig. 5). However, the overall energetically favorable exothermic steps of M1–M2 and M3–M4 more than compensates for the energetically uphill steps of M0–M1 and M2–M3 and helps to drive the reaction towards 1-hexene formation. It is clear from Fig. 5, that the first step of formation of chromacyclopentane M1, by the oxidative coupling of two ethylenes via transition state MTS1 (cf. Scheme 5), has the highest activation barrier of 24.53 kcal/mol, and is therefore the rate determining step (RDS) for the cationic metallacycle pathway. This result from our computational work again is in accordance with the experimental findings of Overett et al. in Cr-based ethylene tetramerization [44]. However, our result markedly differs from the computational findings of Janse van Rensburg et al. who, for a notably different ligand system, find metallacycle growth step as the RDS for Cr-catalyzed ethylene trimerization [49].

The final step of chromacycloheptane, M3(≡C5) converting to 1-hexene bound Cr(II) complex, M4(≡C6), via transition state, MTS3(≡CTS5) is the same as the corresponding step for cationic Cossee pathway and as already discussed, involves a Cr-mediated, concerted 3,7-H shift. This metal mediated hydride shift occurs in a fully concerted fashion via transition state MTS3 in our reaction path (cf. Scheme 5). Recent experimental results [28] also support a concerted mechanism that bypasses the formation of a chromium hydride (Scheme 2a). The concerted mechanism is probably assisted by agostic interactions from 3-CH_2 position to the 7-CH_2 of the metallacycle framework.

4. Conclusions

The selective route to ethylene tri- and tetra-merization using Cr catalysts is an area of much current interest and on the basis of mainly experimental and some computational work it is generally assumed that a metallacycle mechanism is involved [1–40,43,44,49,63,62]. The importance of chlorinated Cr-based active catalysts in these reactions is well known [25]. Therefore, in this work, using minimal ligand framework of chlorides and both cationic and neutral model systems, we have carried out DFT based investigations on Cossee and metallacycle mechanisms for the trimerization of ethylene. Our computational results are in good agreement with several recent experimental results [20] in favor of the cationic Cr(II)–Cr(IV) mechanistic cycle.

Our key findings are:

(a) Formation of chromacyclopentane which is generally accepted to be the starting point for chain growth is not the rate determining step for either of the Cossee mechanisms. In the Cossee pathways the conversion of metallacyclopentanes to the corresponding β-H transferred intermediates are the rate determining steps. The activation barrier of RDS for the cationic path (32.52 kcal/mol) is the highest, and is higher by 3.19 kcal/mol than that for the neutral model. These results are consistent with the experimental observation that butene formation is not a facile reaction with Cr-based catalytic systems.

(b) With neutral intermediates the metallacycle mechanism is not feasible, but with cationic intermediates the formation of chromacyclopentane is the rate determining step. This is in agreement with literature reported experimental work of Overett et al on ethylene tetramerization [44] but different from the computational findings of Janse van Rensburg et al., who for a different ligand system found the metallacycle growth step as the RDS for ethylene trimerization [49]. The activation barrier of the RDS (24.53 kcal/mol) is considerably less than that of the neutral or the cationic Cossee pathways.

With cationic intermediates, the metallacycle mechanism is therefore energetically overwhelmingly preferred over the Cossee mechanism. This is in excellent agreement with most of the recent experimental results in this area [7,20,21,28–30,43,44]. It may be noted that all the experimental results utilize different substituted PNP, SNS, NNN and other complicated ligands on chromium center. Whereas, we have achieved the same results through computational methods using the simplest bare ligand framework of only chlorides on Cr in our model systems.

(c) As our neutral model intermediates fail to follow the metallacycle pathway, Cossee mechanism in such systems is a definite possibility. This provides a plausible explanation for the presence of Cossee mechanism along with many others in Cr-based heterogeneous catalytic systems where no co-catalyst is used, and co-catalyst assisted cationic intermediates formation is ruled out. The experimentally observed critical influence of the co-catalyst on the performance of the homogeneous systems may also be rationalized by invoking the same reasoning.

Acknowledgements

Authors are grateful to Professor S.R. Gadre, University of Pune, India for providing computer facility. Financial support for this work was provided by Reliance Industries Limited. We thank the referees for useful suggestions.

Appendix A. Supplementary material

Supplementary data associated with this article can be found, in the online version, at doi:10.1016/j.jorganchem.2008.12.012.

References

[1] J.W. Freeman, J.L. Buster, R.D. Knudsen, US Patent 5,856,257, Philips Petroleum Company, January 5, 1999.
[2] W.K. Reagan, T.M. Pettijohn, J.W. Freeman, E.A. Benham, US Patent 5786431, Phillips Petroleum Company, 1998.
[3] M.E. Lashier, EP 0780353A1, Phillips Petroleum Company, 1997.
[4] W.K. Reagen, B.K. Conroy, Canadian Patent 2020509, Phillips Petroleum Company, 1991.
[5] W.K. Reagan, T.M. Pettijohn, J.W. Freeman, US Patent 5523507, Phillips Petroleum Company, 1996.
[6] A. Carter, S.A. Cohen, N.A. Cooley, A. Murphy, J. Scutt, D.F. Wass, Chem. Commun. (2002) 858.
[7] T. Agapie, S.L. Schofer, J.A. Labinger, J.E. Bercaw, J. Am. Chem. Soc. 126 (2004) 1304.
[8] D.S. McGuinness, P. Wasserscheid, W. Keim, C. Hu, U. Englert, J.T. Dixon, C. Grove, Chem. Commun. (2003) 334.
[9] J.T. Dixon, J.J.C. Grove, P. Wasserscheid, D.S. McGuinness, F.M. Hess, H. Maumela, D.H. Morgan, A. Bollmann, WO 03053891A1, Sasol Technology, 2003.
[10] J.T. Dixon, P. Wasserscheid, D.S. McGuinness, F.M. Hess, H. Maumela, D.H. Morgan, A. Bollmann, WO 03053890A1, Sasol Technology, 2003.
[11] D.S. McGuinness, P. Wasserscheid, W. Keim, D.H. Morgan, J.T. Dixon, A. Bollmann, H. Maumela, F.M. Hess, U. Englert, J. Am. Chem. Soc. 125 (2003) 5272.
[12] K. Blann, A. Bollmann, J.T. Dixon, A. Neveling, D.H. Morgan, H. Maumela, E. Killian, F.M. Hess, S. Otto, L. Pepler, H.A. Mahomed, M.J. Overett, M.J. Green, WO 04056478A1, Sasol Technology, 2004.
[13] J.T. Dixon, M.J. Green, F.M. Hess, D.H. Morgan, J. Organomet. Chem. 689 (2004) 3641–3668.

[14] D.F. Wass, Dalton Trans. (2007) 816–819.
[15] K. Blann, A. Bollmann, J.T. Dixon, F.M. Hess, E. Killian, H. Maumela, D.H. Morgan, A. Neveling, S. Otto, M.J. Overett, Chem. Commun. (2005) 620–621.
[16] M.J. Overett, K. Blann, A. Bollmann, J.T. Dixon, F. Hess, E. Killian, H. Maumela, D.H. Morgan, A. Neveling, S. Otto, Chem. Commun. (2005) 622–624.
[17] H. Mahomed, A. Bollmann, J.T. Dixon, V. Gokul, L. Griesel, C. Grove, F. Hess, H. Maumela, L. Pepler, Appl. Catal. A: Gen. 255 (2003) 355.
[18] S. Kuhlmann, K. Blann, A. Bollmann, J.T. Dixon, E. Killian, M.C. Maumela, H. Maumela, D.H. Morgan, M. Prétorius, N. Taccardi, P. Wasserscheid, J. Catal. 245 (2007) 279.
[19] D.S. McGuinness, P. Wasserscheid, D.H. Morgan, J.T. Dixon, Organometallics 24 (2005) 552.
[20] D.S. McGuinness, D.B. Brown, R.P. Tooze, F.M. Hess, J.T. Dixon, A.M.Z. Slawin, Organometallics 25 (2006) 3605. and refs therein.
[21] D.S. McGuinness, M. Overett, R.P. Tooze, K. Blann, J.T. Dixon, A.M.Z. Slawin, Organometallics 26 (2007) 1108.
[22] A.K. Tomov, J.J. Chirinos, R.J. Long, V.C. Gibson, M.R.J. Elsegood, J. Am. Chem. Soc. 128 (2006) 7704–7705.
[23] A.K. Tomov, J.J. Chirinos, D.J. Jones, R.J. Long, V.C. Gibson, J. Am. Chem. Soc. 127 (2005) 10166–10167.
[24] D.S. McGuinness, A.J. Rucklidge, R.P. Tooze, A.M.Z. Slawin, Organometallics 26 (2007) 2561–2569.
[25] B. Blom, G. Klatt, J.C.Q. Fletcher, J.R. Moss, Inorg. Chim. Acta 360 (2007) 2890–2896.
[26] D.S. McGuinness, J.A. Suttil, M.G. Gardiner, N.W. Davies, Organometallics 27 (2008) 4238–4247.
[27] E. Groppo, C. Lamberti, S. Bordiga, G. Spoto, A. Zecchina, Chem. Rev. 105 (2005) 115–183.
[28] T. Agapie, J.A. Labinger, J.E. Bercaw, J. Am. Chem. Soc. 129 (2007) 14281. and references therein.
[29] T. Agapie, M.W. Day, L.M. Henling, J.A. Labinger, J.E. Bercaw, Organometallics 25 (2006) 2733–2742.
[30] A. Jabri, C. Temple, P. Crewdson, S. Gambarotta, I. Korobkov, R. Duchateau, J. Am. Chem. Soc. 128 (2006) 9238–9247.
[31] R.D. Köhn, D. Smith, M.F. Mahon, M. Prinz, S. Mihan, G. Kociok-Köhn, J. Organomet. Chem. 683 (2003) 200.
[32] D.H. Morgan, S.L. Schwikkard, J.T. Dixon, J.J. Nair, R. Hunter, Adv. Synth. Catal. 345 (2003) 1.
[33] A. Jabri, P. Crewdson, S. Gambarotta, I. Korobkov, R. Duchateau, Organometallics 25 (2006) 715.
[34] R.D. Kohn, Angew. Chem., Int. Ed. 46 (2007) 2–5.
[35] C. Temple, A. Jabri, P. Crewdson, S. Gambarotta, I. Korobkov, R. Duchateau, Angew. Chem. 118 (2006) 7208–7211.
[36] C. Temple, A. Jabri, P. Crewdson, S. Gambarotta, I. Korobkov, R. Duchateau, Angew. Chem., Int. Ed. 45 (2006) 7050–7053.
[37] S.J. Schofer, M.W. Day, L.M. Lawrence, J.A. Labinger, J.E. Bercaw, Organometallics 25 (2006) 2743–2749.
[38] L.E. Bowen, M.F. Haddow, A.G. Orpen, D.F. Wass, Dalton Trans. (2007) 1160–1168.
[39] A.J. Rucklidge, D.S. McGuinness, R.P. Tooze, A.M.Z. Slawin, J.D.A. Pelletier, M.J. Hanton, P.B. Webb, Organometallics 26 (2007) 2782–2787.
[40] C.N. Temple, S. Gambarotta, I. Korobkov, R. Duchateau, Organometallics 26 (2007) 4598–4603.
[41] P. Cossee, J. Catal. 3 (1964) 65.
[42] E.J. Arlman, P. Cossee, J. Catal. 3 (1964) 80. 89, 99.
[43] A. Bollmann, K. Blann, J.T. Dixon, F.M. Hess, E. Killian, H. Maumela, D.S. McGuinness, D.H. Morgan, A. Neveling, S. Otto, M. Overett, A.M.Z. Slawin, P. Wasserscheid, S. Kuhlmann, J. Am. Chem. Soc. 126 (2004) 14712.
[44] M.J. Overett, K. Blann, A. Bollmann, J.T. Dixon, D. Haasbroek, E. Killian, H. Maumela, D.S. McGuinness, D.H. Morgan, J. Am. Chem. Soc. 127 (2005) 10723. and references therein.
[45] R. Emrich, O. Heinemann, P.W. Jolly, C. Krueger, G.P.J. Verhovnik, Organometallics 16 (1997) 1511–1513.
[46] P.W. Jolly, Acc. Chem. Res. 29 (1996) 544.
[47] M. Peuckert, W. Keim, Organometallics 2 (1983) 594–597.
[48] P. Kuhn, D. Semeril, D. Matt, M.J. Chelcuti, P. Lutz, Dalton Trans. (2007) 515–528.
[49] W. Janse van Rensburg, C. Grove, J.P. Steynberg, K.B. Stark, J.J. Huyser, P.J. Steynberg, Organometallics 23 (2004) 1207. and references therein.
[50] A.N.J. Blok, P.H.M. Budzelaar, A.W. Gal, Organometallics 22 (2003) 2564.
[51] T.J.M. de Bruin, L. Magna, P. Raybaud, H. Toulhoat, Organometallics 22 (2003) 3404.
[52] S. Tobisch, T. Ziegler, Organometallics 22 (2003) 5392.
[53] Z.-X. Yu, K.N. Houk, Angew. Chem., Int. Ed. 42 (2003) 808.
[54] C. Andes, S.B. Harkins, S. Murtuza, K. Oyler, A. Sen, J. Am. Chem. Soc. 123 (2001) 7423.
[55] P.J.W. Deckers, B. Hessen, J.H. Teuben, Organometallics 21 (2002) 5122.
[56] P.J.W. Deckers, B. Hessen, J.H. Teuben, Angew. Chem., Int. Ed. 40 (2) (2001) 2516.
[57] P.J.W. Deckers, B. Hessen, WO 02/066404 (Stichting Dutch Polymer Institute), August 29, 2002.
[58] P.J.W. Deckers, B. Hessen, WO 02/066405 (Stichting Dutch Polymer Institute), August 29, 2002.
[59] S. Tobisch, T. Ziegler, Organometallics 24 (2005) 256–265.
[60] S. Tobisch, T. Ziegler, Organometallics 23 (2004) 4077–4088.
[61] S. Tobisch, T. Ziegler, J. Am. Chem. Soc. 126 (2004) 9059–9071.
[62] P.R. Elowe, C. McCann, P.G. Pringle, S.K. Spitzmesser, J.E. Bercaw, Organometallics 25 (2006) 5255–5260.
[63] W. Janse van Rensburg, J.-A.V. den Berg, P.J. Steynberg, Organometallics 26 (2007) 1000–1013.
[64] A.D. Becke, Phys. Rev. A 38 (1988) 3098.
[65] C. Lee, W. Yang, R.G. Parr, Phys. Rev. B 37 (1988) 785.
[66] A.D. Becke, J. Chem. Phys. 98 (1993) 5648.
[67] C.E. Check, T.O. Faust, J.M. Bailey, B.J. Wright, T.M. Gilbert, L.S. Sunderlin, J. Phys. Chem. A 105 (2001) 8111–8116.
[68] T.J. Dines, S. Inglis, Phys. Chem. Chem. Phys. 5 (2003) 1320–1328.
[69] M.J. Frisch, G.W. Trucks, H.B. Schlegel, G.E. Scuseria, M.A. Robb, J.R. Cheeseman, V.G. Zakrzewski, J.A. Montgomery Jr., R.E. Stratmann, J.C. Burant, S. Dapprich, J.M. Millam, A.D. Daniels, K.N. Kudin, M.C. Strain, O. Farkas, J. Tomasi, V. Barone, M. Cossi, R. Cammi, B. Mennucci, C. Pomelli, C. Adamo, S. Clifford, J. Ochterski, G.A. Petersson, P.Y. Ayala, Q. Cui, K. Morokuma, P. Salvador, J.J. Dannenberg, D.K. Malick, A.D. Rabuck, K. Raghavachari, J.B. Foresman, J. Cioslowski, J.V. Ortiz, A.G. Baboul, B.B. Stefanov, G. Liu, A. Liashenko, P. Piskorz, I. Komaromi, R. Gomperts, R.L. Martin, D.J. Fox, T. Keith, M.A. Al-Laham, C.Y. Peng, A. Nanayakkara, M. Challacombe, P.M.W. Gill, B. Johnson, W. Chen, M.W. Wong, J.L. Andres, C. Gonzalez, M. Head-Gordon, E.S. Replogle, J.A. Pople, GAUSSIAN 98, Revision A.11, Gaussian Inc., Pittsburgh PA, 2001.
[70] A.C. Filippou, S. Schneider, G. Schnakenburg, Angew. Chem., Int. Ed. 42 (2003) 4486–4489.
[71] R. Bau, R.G. Teller, S.W. Kirtley, T.F. Koetzle, Acc. Chem. Res. 12 (1979) 176–183.
[72] MDS 3.5: Molecular Design Suite, VLife Sciences Technologies Pvt. Ltd., Pune, India, 2008.